Competitive Triplex/Quadruplex Equilibria Involving Guanine-Rich Oligonucleotides†

Wendy M. Olivas and L. James Maher, III*

Eppley Institute for Research in Cancer and Allied Diseases and the Department of Biochemistry and Molecular Biology, University of Nebraska Medical Center, 600 South 42nd Street, Omaha, Nebraska 68198-6805

Received August 30, 1994; Revised Manuscript Received October 24, 1994®

ABSTRACT: Oligonucleotide-directed triple helix formation in the purine motif involves the binding of guanine-rich oligonucleotides to duplex DNA. Although this approach has been proposed for *in vivo* gene inhibition, triple helix formation by guanine-rich oligonucleotides is severely inhibited by physiological concentrations of certain monovalent cations (M^+), especially K^+. To clarify the mechanism of this inhibition, electrophoretic gel mobility shift titrations were performed to analyze the formation and stability of a purine motif triple helix in the presence of M^+ and to monitor oligonucleotide aggregation under these conditions. M^+ inhibition of triplex formation exhibited a concentration and ionic radius dependence that correlates with the ability of M^+ to stabilize guanine quartet structures. In the presence of inhibitory [M^+], guanine-rich oligonucleotides formed aggregates having characteristics consistent with the involvement of guanine quartets. The inhibitory effects of K^+ on triplex formation could not be reversed by addition of the physiological polyamines spermidine^{3+} or spermine^{4+}. M^+ reduced the equilibrium concentration of the triplex primarily by decreasing the rate of triplex formation, but M^+ also caused a detectable increase in the rate of triplex dissociation. Together, these results suggest that triplex inhibition under physiological ionic conditions is caused by competing equilibria wherein guanine-rich oligonucleotides form aggregates involving guanine quartets. Approaches to destabilizing aggregates of guanine-rich oligonucleotides under physiological conditions will be required before *in vivo* applications can be realistically considered.

Oligonucleotide-directed triple helix formation provides a potential strategy for designing artificial gene repressors (Moser & Dervan, 1987; Cooney et al., 1988; Maher, 1992; Hélène, 1991). Triple helix formation involves site-specific recognition of duplex DNA by hydrogen bonding between oligonucleotide bases and purine bases in the major groove. Triple helix formation occurs in two distinct patterns termed the pyrimidine motif and the purine motif (Maher, 1992). In the pyrimidine motif, oligonucleotides bind parallel to the purine strand of the duplex by Hoogsteen hydrogen bonding (T•A•T and C^+•G•C triplets; Moser & Dervan, 1987). In the purine motif, oligonucleotides bind antiparallel to the purine strand of the duplex by reverse Hoogsteen hydrogen bonding (T•A•T or A•A•T and G•G•C triplets; Beal & Dervan, 1991).

Because the pyrimidine motif requires slightly acidic pH to promote protonation of oligonucleotide cytosines (Moser & Dervan, 1987; Povsic & Dervan, 1989; Singleton & Dervan, 1992), the pH-independent purine motif has been thought to be a more viable approach for *in vivo* applications (Cooney et al., 1988; Postel et al., 1991; Orson et al., 1991; Ing et al., 1993). However, this report and two previous studies indicate that oligonucleotide-directed triple helix formation in the purine motif is inhibited by physiological concentrations of certain monovalent cations (M^+),[1] especially K^+ (Milligan et al., 1993; Cheng & Van Dyke, 1993). The mechanism of this inhibition remains unclear. It has been established that K^+ can stabilize intermolecular structures involving G/T-rich oligonucleotides, presumably by coordination between guanines in stacked quartets (Williamson et al., 1989; Sen & Gilbert, 1990; Laughlan et al., 1994). However, other data suggest that M^+ inhibit triple helix formation in the purine motif by a mechanism that does not involve promotion of guanine quartets (Cheng & Van Dyke, 1993). An understanding of triple helix formation by guanine-rich oligonucleotides under physiological ionic conditions will be critical for judging the therapeutic potential of this strategy.

Here we report the results of electrophoretic gel mobility shift titrations that analyzed the formation and stability of a purine motif triple helix in the presence of M^+ and monitored oligonucleotide aggregation under these conditions. Several conclusions are presented. First, formation of purine motif triplexes was dramatically inhibited by physiological concentrations of Na^+ and K^+. The concentration and ionic radius dependence of inhibition by these and other M^+ correlated with the ability of these M^+ to stabilize guanine quartet structures (Guschlbauer et al., 1990). Second, in the presence of inhibitory M^+ concentrations, guanine-rich oligonucleotides formed aggregates having characteristics consistent with the involvement of guanine quartets. Third, the inhibitory effects of K^+ on triplexes could no be re-

† Supported in part by Grant 5 P30 CA36727-08 from the National Cancer Institute and Grant GM 47814 from the National Institutes of Health. L.J.M. is a recipient of a Junior Faculty Research Award from the American Cancer Society and a Young Investigator's Award from Abbott Laboratories. W.M.O. is supported by a University of Nebraska Medical Center Emley Fellowship.

* To whom correspondence should be addressed: 402-559-8288 (voice), 402-559-4651 (FAX), jmaher@unmc.edu (Internet).

® Abstract published in *Advance ACS Abstracts,* December 1, 1994.

[1] Abbreviations: M^+, monovalent cation(s); cpm, radioactive counts per minute; Tris-HCl, 2-amino-2-(hydroxymethyl)-1,3-propanediol hydrochloride.

0006-2960/95/0434-278$09.00/0

A.

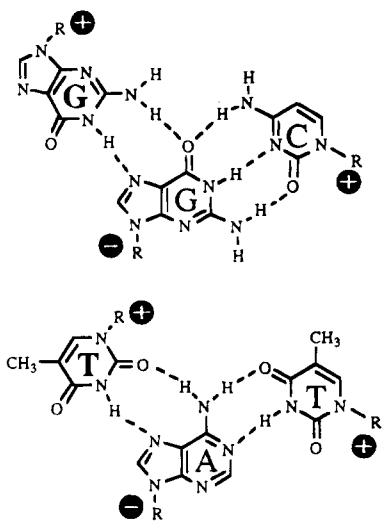

B.

```
          3' GGGTGGGTGGTGGG          1
5' GATCCGCGTGGGAGGGAGGAGGGCCCGGATC   2
3' CTAGGCGCACCCTCCCTCCTCCCGGGCCTAG   3

       3' Biotin-GGGTGGGTGGTGGG      1B

          5' CCCACCCACCACCC          4
```

FIGURE 1: (A) DNA triple helix formation in the purine motif. G·G·C and T·A·T base triplets are involved in duplex DNA recognition by guanine-rich oligonucleotides (bold). Filled circles indicate strand polarities. (B) Experimental design. The duplex target sequence is formed by annealing complementary oligonucleotides **2** and **3**. Oligonucleotide **1** binds in the major groove of the duplex, antiparallel to oligonucleotide **2**. Oligonucleotide **1B** (containing a 3′ biotin) was synthesized using a commercial biotin C7 CPG support (Glen Research). Oligonucleotide **4** is complementary to **1**.

versed by addition of the physiological polyamines spermidine^{3+} or spermine^{4+}. Finally, M^+ primarily reduced the equilibrium concentration of the triplex by decreasing its rate of formation, but M^+ also caused a detectable increase in the rate of triplex dissociation. Together, these results suggest that triplex inhibition under physiological ionic conditions is caused by the existence of competing equilibria wherein guanine-rich oligonucleotides form aggregates involving guanine quartets.

MATERIALS AND METHODS

Oligonucleotides. Oligonucleotide sequences are shown in Figure 1. Oligonucleotides were synthesized by phosphoramidite chemistry on an ABI Model 380B DNA synthesizer, purified by denaturing polyacrylamide gel electrophoresis, eluted from gel slices, desalted by Sep-Pak C_{18} cartridge chromatography (Waters), and quantitated by absorbance at 260 nm using molar extinction coefficients (M^{-1} cm^{-1}) of 15 400 (A), 11 700 (G), 7300 (C), and 8800 (T), assuming no hypochromicity. Oligonucleotides comprising the target duplex were annealed as follows: 500 pmol each of oligonucleotides **2** and **3** (initially lacking four 3′ nucleotides relative to Figure 1B) was mixed with 2 μL of 5 M NaCl and brought to a total volume of 42 μL with H_2O. This annealing reaction mixture was incubated at 75 °C for 12 min and then gradually cooled to 25 °C. Sixty picomoles of the resulting oligonucleotide duplex was radiolabeled using Klenow fragment of DNA polymerase I and [α-^{32}P]-dATP in the presence of 2 mM dGTP, dTTP, and dCTP. The labeled duplex was purified by native polyacrylamide gel electrophoresis, eluted from the gel, extracted with phenol/chloroform/isoamyl alcohol (25:24:1), precipitated with ethanol in the presence of sodium acetate, and resuspended in H_2O. To radiolabel oligonucleotide **1**, 10 pmol of **1** was treated with T4 polynucleotide kinase in the presence of [γ-^{32}P]ATP and then precipitated from ethanol in the presence of ammonium acetate.

Electrophoretic Mobility Shift Assays. For triplex assays in which [**1**] varied and [M^+] remained constant, binding reaction mixtures contained (in order of addition) H_2O, labeled duplex (50 000 cpm; ca. 0.02 pmol), 1 μL of 10× binding buffer (250 mM Tris-HCl, pH 8.0, and 60 mM $MgCl_2$), 1 μL of 100 mM NaCl or KCl (as indicated), 1 μL of 1 mg/mL yeast tRNA, and 1 μL of **1** (to yield the indicated final concentration) in a final volume of 10 μL. Reaction mixtures were incubated at 22 °C for 5 h and were then supplemented with 1 μL of an 80% glycerol solution containing bromophenol blue. Reactions were analyzed by electrophoresis through 20% native polyacrylamide gels (19:1 acrylamide/bisacrylamide) prepared in 1× TBE (100 mM Tris base, 110 mM boric acid, and 2 mM EDTA) supplemented with 8 mM $MgCl_2$. Electrophoresis was performed in this buffer (with recirculation) at 4 °C overnight (9 V/cm). The resulting gel was imaged and analyzed by storage phosphor technology using a Molecular Dynamics PhosphorImager.

For triplex assays in which [M^+] varied and [**1**] remained constant, binding reaction mixtures contained (in order of addition) H_2O, labeled duplex (50 000 cpm; ca. 0.02 pmol), 1 μL of 10× binding buffer, 1 μL of 1 mg/mL yeast tRNA, 1 μL of stock solution of NaCl, KCl, LiCl, CsCl, RbCl, or NH_4Cl (to yield the indicated final concentration), and 1 μL of 10 μM **1** in a final volume of 10 μL. Reaction mixtures were analyzed as described above.

To analyze aggregation of **1**, binding reaction mixtures contained labeled **1** (50 000 cpm; ca. 0.05 pmol), 1 μL of 10× binding buffer, 1 μL of 1 mg/mL yeast tRNA, 1 μL of 10 μM **1** or 1 μL of 10 μM biotinylated oligonucleotide **1B**, or 0.5 μL of both (as indicated), 2 μL of 1 M NaCl or KCl (as indicated), 1 μL of 10 μM streptavidin (Pierce; as indicated), and H_2O in a final volume of 10 μL. Reaction mixtures were incubated at 22 °C for 4 h and analyzed as described above.

For triplex assays with varying [polyamine], binding reaction mixtures contained (in order of addition) H_2O, labeled duplex (50 000 cpm; ca. 0.02 pmol), 1 μL of 10× binding buffer, 1 μL of 1 mg/mL yeast tRNA, 2 μL of 500 mM NaCl or KCl (as indicated), 1 μL of 10 μM **1**, and 1 μL of spermidine^{3+} or spermine^{4+} solution (to yield the indicated final concentration) in a final volume of 10 μL. Reaction mixtures were analyzed as described above.

For assays monitoring triplex dissociation rates, binding reaction mixtures contained labeled duplex (50 000 cpm; ca. 0.02 pmol), 1 μL of 10× binding buffer, 1 μL of 1 mg/mL yeast tRNA, 1 μL of 10 μM **1**, and H_2O in a final volume of 6.5 μL. Reaction mixtures were incubated at 22 °C for 1 h. One and one-half microliters of 10 μM oligonucleotide **4** or H_2O was added to each reaction mixture as indicated. Reaction mixtures were incubated at 22 °C for 30 min,

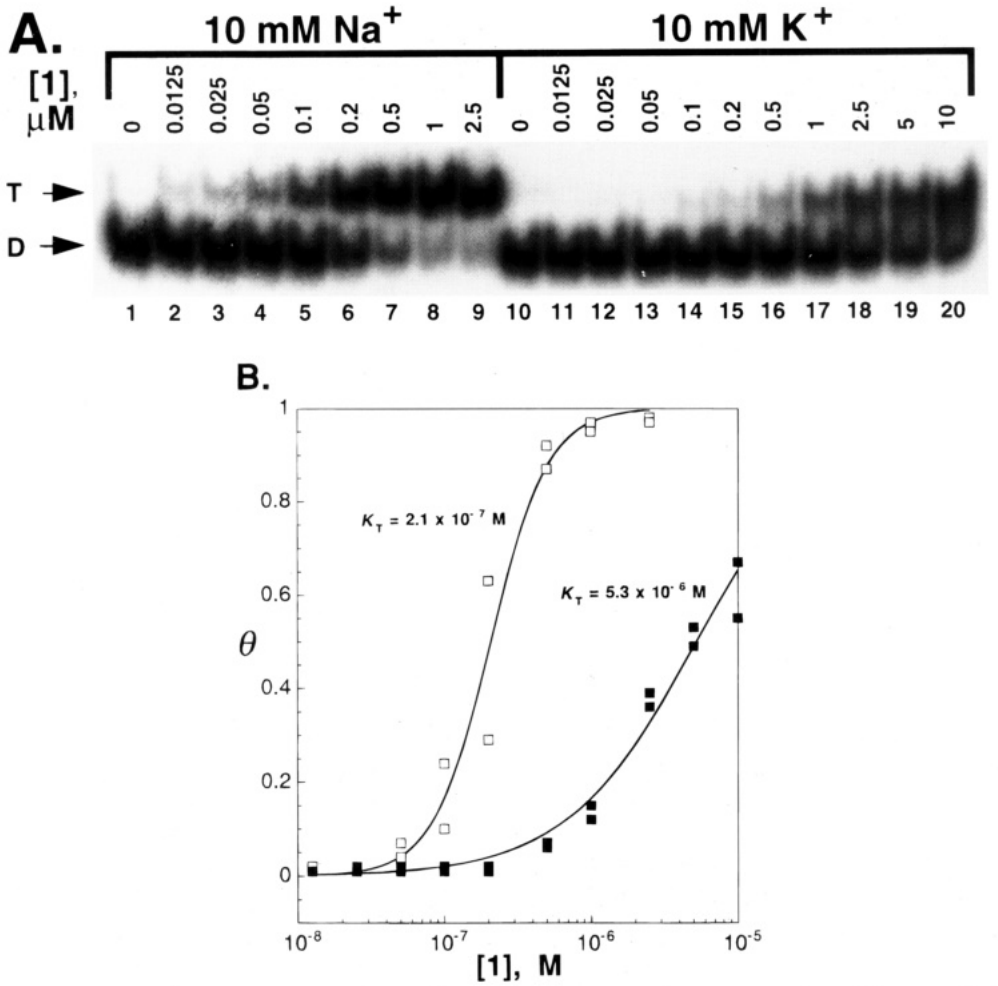

FIGURE 2: Triplex inhibition by K^+. (A) Electrophoretic mobility shift assay. Increasing concentrations of **1** were added to labeled target duplex in the presence of 10 mM Na^+ (lanes 1−9) or 10 mM K^+ (lanes 10−20). Mobilities of free duplex (D) and triplex (T) are indicated. (B) Binding curves for **1** with target duplex in the presence of 10 mM Na^+ (□) or 10 mM K^+ (■) were fitted using data from electrophoretic mobility shift titrations. The fraction of duplex in triplex form (θ) was calculated from eq 1 and fitted to eq 2 to provide estimates of K_T as described in Materials and Methods.

followed by the addition of 2 μL of 500 mM KCl, 500 mM LiCl, or H_2O as indicated. Reaction mixtures were incubated at 22 °C for 1, 2, 3, or 4 h before analysis as described above.

Analysis of Gel Mobility Shift Titrations. The apparent fraction, θ, of target duplex bound by **1** was calculated for each gel lane using the definition

$$\theta = S_{\text{triplex}}/(S_{\text{triplex}} + S_{\text{duplex}}) \quad (1)$$

where S_{triplex} and S_{duplex} represent the storage phosphor signal for triplex and duplex complexes, respectively. Values of the apparent triplex dissociation constant, K_T, were obtained by least squares fitting of the data to the binding isotherm

$$\theta = ([O]^n/K_T^n)/(1 + [O]^n/K_T^n) \quad (2)$$

where [O] is the total concentration of **1**, and n is the Hill coefficient (Cantor & Schimmel, 1980).

Estimates for the apparent dissociation rate constant for triplexes involving **1**, k_{off}, were obtained by least squares fitting of kinetic data to the equation

$$\theta_t/\theta_0 = e^{-k_{\text{off}}t} \quad (3)$$

where t is the time after M^+ addition, θ_t is the apparent fraction of target duplex bound by **1** at time t, and θ_0 is the apparent fraction of target duplex bound by **1** at time zero. Relative k_{off} values were calculated by the equation

$$\text{rel } k_{\text{off}} = k_{\text{off}(M^+)}/k_{\text{off}(0)} \quad (4)$$

where $k_{\text{off}(M^+)}$ is the value of k_{off} for the reaction mixture supplemented with M^+, and $k_{\text{off}(0)}$ is the value of k_{off} for the unsupplemented reaction mixture.

RESULTS

Experimental Design. The model system reported here is based on guanine-rich oligonucleotide **1**, which binds site-specifically to a homopurine sequence in the target duplex according to the purine triple helix motif (Figure 1). Electrophoretic mobility shift assays were used to analyze the formation of both triple helices and aggregates involving **1**.

Triplex Inhibition by M^+. Equilibrium dissociation constants were first measured for triplexes in the presence of subphysiological levels (10 mM) of Na^+ or K^+. Figure 2A presents the results of such an experiment, in which labeled duplex was incubated in the presence of increasing concentrations of **1**. Figure 2B depicts pooled data from two experiments of this type. Values of K_T were calculated as described in Materials and Methods. The value of K_T

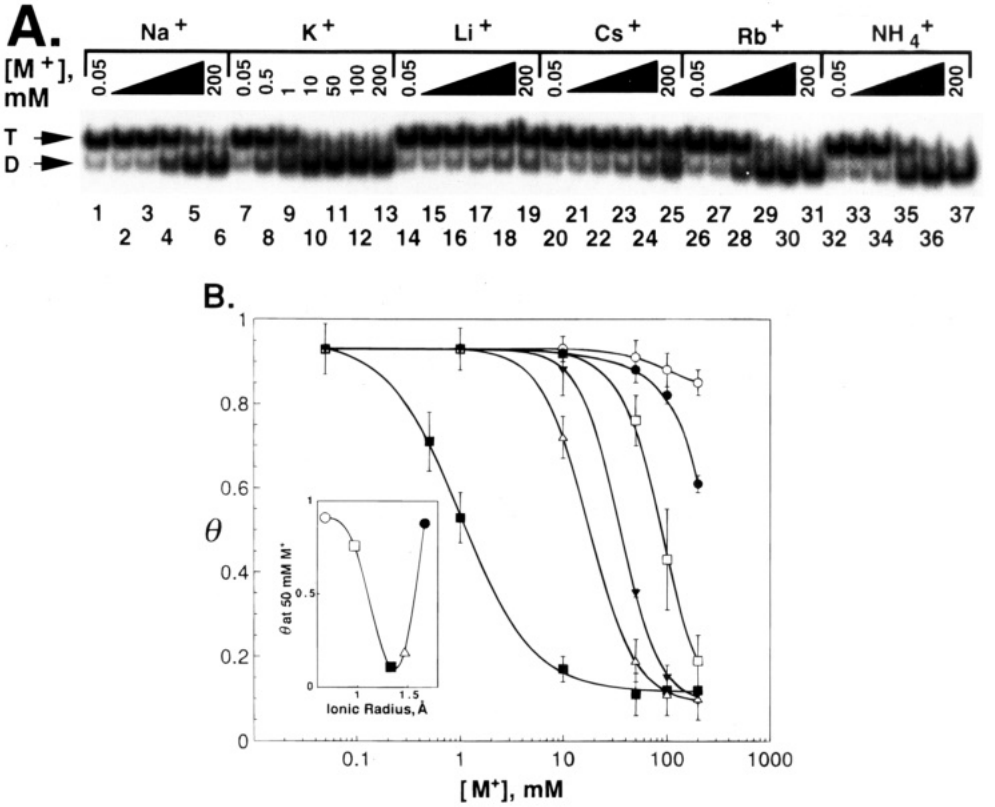

FIGURE 3: Effects of different M^+ on duplex/triplex equilibria. (A) Electrophoretic mobility shift assay. Increasing millimolar concentrations (0.05, 1, 10, 50, 100, 200) of Na^+ (lanes 1−6), K^+ (lanes 7−13), Li^+ (lanes 14−19), Cs^+ (lanes 20−25), Rb^+ (lanes 26−31), and NH_4^+ (lanes 32−37) were added to the labeled target duplex, followed by the addition of 1 μM **1**. Studies with K^+ contained slightly different concentrations, as indicated. Mobilities of free duplex (D) and triplex (T) are indicated. (B) Triplex inhibition curves for 1 μM **1** binding target duplex in the presence of K^+ (■), Rb^+ (△), NH_4^+ (▼), Na^+ (□), Cs^+ (●), or Li^+ (○) were fitted using data from electrophoretic mobility shift titrations. The fraction of duplex in triplex form (θ) was calculated from eq 1 as described in Materials and Methods. The inset depicts θ values at 50 mM alkali metal M^+ versus ionic radius.

[^{32}P]-1 (tracer)	+	+	+	+	+	+	+	+	+	+	+	+	+	+	+	+
Na^+ (200 mM)	+			+	+				+	+			+	+		
K^+ (200 mM)		+				+	+				+	+			+	+
1 (1 μM)			+	+	+	+	+						.5	.5	.5	.5
1B (1 μM)								+	+	+	+	+	.5	.5	.5	.5
streptavidin					+		+			+		+		+		+

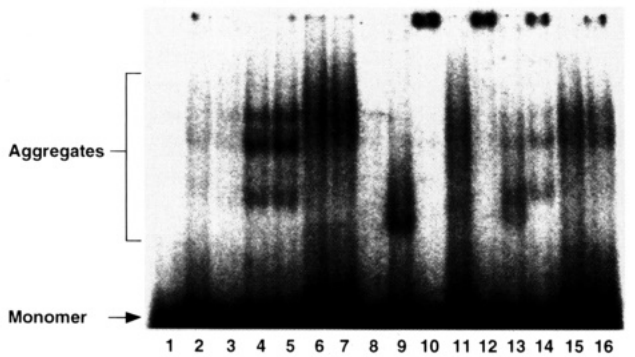

FIGURE 4: Electrophoretic mobility shift assay of **1** aggregates. All reactions contained labeled **1** at trace concentration with other components as indicated. Positions of monomeric and aggregated forms of **1** are indicated.

measured in the presence of 10 mM K^+ (5.3×10^{-6} M) was 25-fold larger than that measured in the presence of 10 mM Na^+ (2.1×10^{-7} M). This striking dependence of K_T on the identity of M^+ was further explored by comparing triplex inhibition by five alkali metal cations as well as NH_4^+. Figure 3A depicts an example of such an experiment, in which the ratios of duplex and triplex species were quantitated at increasing $[M^+]$. Figure 3B depicts the average (±SD) of two such experiments. Triplex inhibition followed the order $K^+ > Rb^+ > NH_4^+ > Na^+ > Cs^+ > Li^+$. The striking agreement between this ranking and the ordering of monovalent ions as stabilizers of guanine quartets (Guschlbauer et al., 1990) suggests the involvement of competing aggregation equilibria involving guanine-rich **1**. When plotted as a function of ionic radius (Figure 3B, inset), the maximum inhibition observed in the presence of K^+ may therefore reflect favorable coordination of K^+ between stacked guanine quartets (Williamson et al., 1989; Sen & Gilbert, 1990).

Aggregation of **1**. To explore the possibility that aggregation of **1** (presumably by formation of guanine quartets) causes triplex inhibition at approximately physiological $[K^+]$, we studied the electrophoretic mobility of **1** in the presence of 200 mM Na^+ or K^+. For both ions, this concentration was sufficient for greater than 80% inhibition of triple helix formation (Figure 3B). When studied at low concentration (~8 nM), labeled **1** remained in monomeric form in the presence of 200 mM Na^+ or K^+ (Figure 4, lanes 1 and 2). In the absence of M^+, **1** also remained in monomeric form at 1 μM concentration (Figure 4, lane 3). However, a change in mobility was observed for a 1 μM concentration of **1** in the presence of 200 mM Na^+ or K^+ (Figure 4, lanes 4 and 6). This apparent concentration dependence of the mobility of **1** suggests the formation of aggregates. Na^+ promoted the formation of three distinct bands of reduced mobility, while the corresponding pattern was less distinct in the presence of K^+ (Figure 4, lanes 4 and 6).

To further clarify whether these retarded species represented single-stranded conformers or multistranded aggregates, oligonucleotide **1B** was designed with the same sequence as **1**, but also containing a 3′ biotin moiety (Figure 1B). In the absence of M^+, labeled **1** remained in monomeric form in the presence of 1 μM **1B** (Figure 4, lane 8). Upon the addition of 200 mM Na^+ to labeled **1** in the presence of 1 μM **1B**, a single shifted species was observed (Figure 4, lane 9). This difference in the mobility of labeled **1** in the presence of 1 μM **1** versus 1 μM **1B** (Figure 4, compare lanes 4 and 9) implies the formation of aggregates involving labeled **1** and excess unlabeled **1** or **1B**. Again, 200 mM K^+ promoted a less distinct pattern of new bands relative to that promoted by 200 mM Na^+ (Figure 4, compare lanes 6 and 11).

Aggregation was proven by showing that labeled **1** became complexed with biotinylated **1B**. The addition of streptavidin (which binds biotin with high affinity and specificity) caused the supershift of previously retarded bands promoted by Na^+ or K^+ (Figure 4, lanes 10 and 12). Although supershifted complexes remained near the origin in 20% gels, they entered 5% gels, migrating as distinct species (data not shown). This supershift effect was not due to nonspecific protein–oligonucleotide interactions, as retarded mobility bands observed in the presence of 1 μM **1** and Na^+ or K^+ were not supershifted (Figure 4, lanes 5 and 7). Reactions containing equimolar (0.5 μM) concentrations of **1** and **1B** in the presence of 200 mM Na^+ or K^+ produced retarded species representing the sum of bands produced with 1 μM **1** and with 1 μM **1B** (Figure 4, lanes 13 and 15). The addition of streptavidin supershifted approximately half of the retarded species promoted by 200 mM Na^+ or K^+ (Figure 4, lanes 14 and 16, respectively). In particular, the Na^+-promoted **1B**-specific species was completely supershifted.

The appearance of intermolecular aggregates in the presence of M^+ suggests that M^+ inhibits triplex formation by stabilizing alternative structures involving **1**. It is possible that the extreme stability of guanine quartets in the presence of K^+ allows persistence of many aggregated species (the observed indistinct bands, e.g., Figure 4, lane 6), while Na^+ is able to promote only the most thermodynamically stable arrangements (the observed distinct bands, e.g., Figure 4, lane 4). Moreover, it is known that non-guanine residues at the termini of guanine-rich oligonucleotides tend to limit the variety of stable aggregates (Sen & Gilbert, 1992; Lu et al., 1992). This phenomenon may explain the simplified aggregation pattern observed for labeled **1** in the presence of Na^+ and 1 μM **1B** (Figure 4, lane 9).

Effect of Polyamines on Duplex/Triplex Equilibria. Intracellular $[K^+]$ is thought to be ~100−200 mM (Alberts et al., 1983). On the basis of the experimental results presented here, such concentrations would be sufficient to almost completely inhibit triplex formation by guanine-rich oligonucleotides. Might physiological concentrations of polyamines such as spermidine^{3+} and spermine^{4+} (~1 mM; Tabor & Tabor, 1976) counter this inhibitory effect? The duplex/triplex equilibrium was quantitated for reactions containing 100 mM Na^+ or K^+, and increasing concentrations of spermidine^{3+} or spermine^{4+}. Results are shown graphically in Figure 5. When tested at 1 mM, spermine^{4+} almost completely reversed the inhibition of triplex formation due to 100 mM Na^+, while spermidine^{3+} only partially reversed this inhibition. In contrast, neither spermine^{4+} nor spermidine^{3+} could reverse the inhibitory effects of 100 mM K^+.

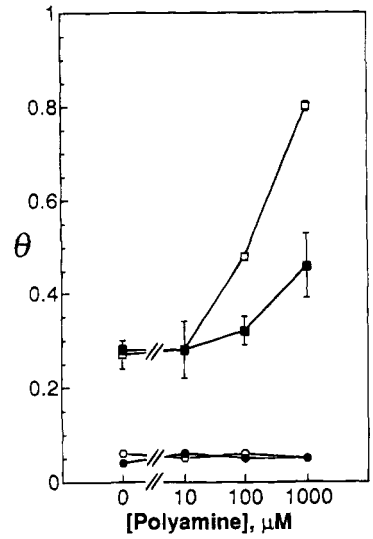

FIGURE 5: Effect of polyamines on duplex/triplex equilibria. Increasing concentrations of spermine^{4+} (□, ○) or spermidine^{3+} (■, ●) were added to reaction mixtures containing labeled target duplex, **1** (1 μM), and Na^+ (100 mM, □, ■) or K^+ (100 mM, ○, ●). The fraction of duplex in triplex form (θ) was calculated from eq 1 as described in Materials and Methods.

Rates of Triplex Dissociation in the Presence of M^+. A previous report indicates that triplex inhibition by K^+ occurs exclusively by slowing triplex formation, rather than by increasing the rate of triplex dissociation (Cheng & Van Dyke, 1993). To explore this proposition with the present model system, 100 mM Li^+ or K^+ or H_2O was added to preformed triplexes. The ratios of triplex and duplex species were then quantitated at hourly time points after M^+ addition. Results of this experiment are shown graphically in Figure 6A. The triplex/duplex equilibrium shifted more rapidly toward the duplex in the presence of K^+ than in the presence of Li^+ or in the absence of added M^+. This result suggested the possibility of an increased triplex dissociation rate in the presence of K^+.

To measure the apparent triplex dissociation rate constant in the absence of a reassociation reaction, oligonucleotide **4** (complementary to **1**) was prepared. Sufficient **4** was added to preformed triplexes to sequester free **1**. Preformed triplexes were then supplemented with H_2O or 100 mM Li^+ or K^+. Triplex and duplex species were quantitated at hourly time points thereafter. Results of these experiments are shown graphically in Figure 6B. Apparent dissociation rate constants were calculated as described in Materials and Methods and are listed in Table 1. Under these conditions, triplexes dissociated 2.9-fold faster in the presence of Li^+ than in the H_2O control, and triplexes dissociated 7.2-fold faster in the presence of K^+ than in the H_2O control. Thus, although the predominant effect of M^+ is to reduce the rate of triple helix formation, M^+ detectably increased triplex dissociation rates in this system.

DISCUSSION

Formation of a triple-helical DNA structure involving a guanine-rich oligonucleotide was strongly inhibited by physiological K^+ concentrations. The concentration and ionic radius dependence of inhibition by a series of M^+ implicate

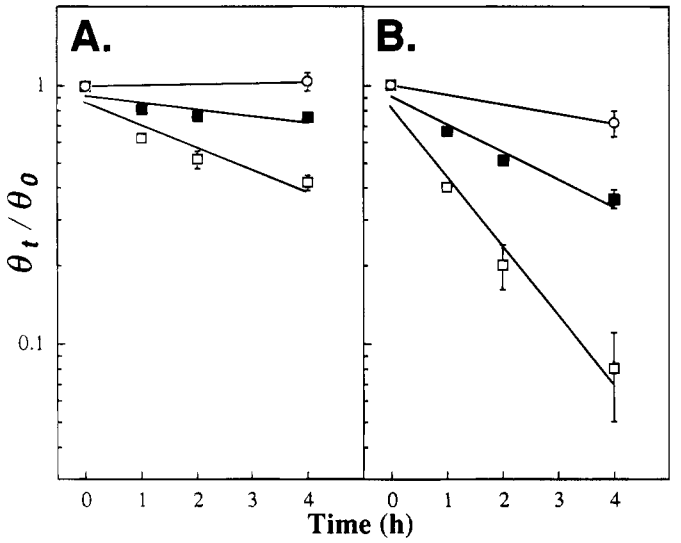

FIGURE 6: Dissociation rates for triplexes in the presence of M^+. Reaction mixtures containing labeled target duplex and 1 μM **1** were incubated for 1 h, followed by the addition of a 1.5-fold excess of **4** (panel B) or no addition of **4** (panel A). Li^+ (100 mM, ■), K^+ (100 mM, □), or H_2O (○) was then added, and reaction mixtures were allowed to incubate for 1, 2, 3, or 4 h before electrophoretic analysis. The fractions of duplex in triplex form at time zero (θ_0) and at each time point (θ_t) were calculated from eq 1, and θ_t/θ_0 values were fitted to eq 3 as described in Materials and Methods.

Table 1: Comparison of k_{off} Values Obtained from Figure 6A[a]

$[M^+]$, M	k_{off} (s^{-1})	rel k_{off}
	2.4×10^{-5}	1
0.1 (Li^+)	6.8×10^{-5}	2.9
0.1 (K^+)	1.7×10^{-4}	7.2

[a] Values of k_{off} were calculated from eq 3 as described in Materials and Methods. Relative k_{off} values were calculated from eq 4 as described in Materials and Methods.

guanine quartets in a competing aggregation equilibrium involving the guanine-rich oligonucleotide. It is proposed that M^+ (particularly K^+) inhibit triplexes by stabilizing alternative guanine quartet structures involving **1**. This proposal can be summarized in terms of two equilibria that compete for **1**:

$$p\mathbf{1} + qM^+ \rightleftharpoons \mathbf{1}_{agg} \quad (5)$$

$$\mathbf{1} + D + mM^{2+} \rightleftharpoons T + nM^+ \quad (6)$$

where $\mathbf{1}_{agg}$ is **1** in aggregated form(s), m, n, p, and q are stoichiometric coefficients, D is duplex, and T is triplex. Equation 5 presents a general view of the aggregation equilibrium for **1**. The value of p is unknown. For intermolecular quadruplex formation, the expected value of p would be 4, but it is possible that guanine quartets are formed from combinations of four aligned, parallel strands of **1**, a dimer of **1** hairpins, or an arrangement of unaligned strands of **1**. The formation of hairpin structures seems unlikely for **1** (14 nt), though this possibility cannot be ruled out. The presence of multiple species of K^+-promoted aggregates suggests a combination of four-stranded guanine quartets aligned in different registers. In contrast, the single Na^+-promoted aggregate band observed in the presence of excess **1B** may represent a stable quadruplex formed from four aligned, parallel oligonucleotides. Definitive assignments of observed aggregate bands must await further analyses such as dimethyl sulfate footprinting to determine which guanine N7 groups are protected.

The proposed existence of competing triplex versus quadruplex equilibria predicts that triplex inhibition by M^+ should occur primarily by a reduction in the rate of triple helix formation, as has previously been suggested (Cheng & Van Dyke, 1993). However, the data presented here also show that the presence of Li^+ detectably increases the apparent rate of triplex dissociation, and the effect is more dramatic for K^+. Equation 6 takes into account the likely uptake of M^{2+} and the corresponding release of M^+ upon triple helix formation. It has previously been established that 0.2−0.6 M Na^+ can destabilize triplexes, presumably by the displacement of triplex-stabilizing M^{2+} (Maher et al., 1990). This phenomenon requires high $[M^+]$ and does not appear consistent with the differential effects on triplex dissociation rates observed for Li^+ and K^+. An alternative mechanism could involve traces of single-stranded **1** that may, in the presence of M^+, actively promote removal of duplex-bound **1** into guanine quartet structures.

The current results can be compared and contrasted with a recent study of triplex inhibition by M^+ (Cheng & Van Dyke, 1993). Identical orderings for ion-specific triplex inhibition were reported. Curiously, however, no evidence was observed in the previous study to suggest the involvement of multistranded aggregates of the guanine-rich oligonucleotide under study (5′-$TG_3TG_4TG_4TG_3T$). It was hypothesized that M^+ inhibited a putative isomerization of the oligonucleotide into a conformation somehow required for triplex formation. In addition, little effect on triplex dissociation rates was reported in the presence of M^+. It remains unclear why the guanine-rich oligonucleotide studied in the previous report failed to display intermolecular aggregation as is evident here for **1**. The present results favor quartet-mediated aggregation as the most plausible explanation for inhibition of purine motif triple helices by M^+ (particularly K^+).

These results have significant implications for proposed *in vivo* therapeutic applications of guanine-rich oligonucleotides. Most importantly, current designs for oligonucleotide drugs intended to recognize duplex DNA using the purine motif appear unlikely to permit triple helix formation with target chromosomal DNA under cellular ionic conditions

(where K^+ is the relevant cation). Even the preassembly of triplexes for *in vitro* assays may not prevent dissociation induced by M^+. These significant obstacles for DNA recognition in the purine motif might be addressed by new oligonucleotide designs. For example, when tested in the presence of 140 mM KCl, a guanine-rich oligonucleotide containing 7-deaza-2′-deoxyxanthosine substituted for T showed 100-fold greater affinity for its duplex DNA target than the unmodified oligonucleotide (Milligan et al., 1993). The role of competing triplex/quadruplex equilibria in this enhancement remains to be elucidated. Approaches to destabilizing aggregates of guanine-rich oligonucleotides under physiological conditions will be required before *in vivo* applications can be realistically considered.

ACKNOWLEDGMENT

We acknowledge the excellent technical assistance of D. Eicher and C. Mountjoy. We thank C. Price for comments on the manuscript and W. Braunlin for helpful discussion.

REFERENCES

Alberts, B., Bray, D., Lewis, J., Raff, M., Roberts, K., & Watson, J. D. (1983) in *Molecular Biology of The Cell*, p 286, Garland Publishing, Inc., New York.

Beal, P. A., & Dervan, P. B. (1991) *Science 251*, 1360−1363.

Cantor, C. R., & Schimmel, P. R. (1980) in *Biophysical Chemistry*, p 864, W. H. Freeman and Company, New York.

Cheng, A.-J., & Van Dyke, M. W. (1993) *Nucleic Acids Res. 21*, 5630−5635.

Cooney, M., Czernuszewicz, G., Postel, E. H., Flint, S. J., & Hogan, M. E. (1988) *Science 241*, 456−459.

Guschlbauer, W., Chantot, J.-F., & Thiele, D. (1990) *J. Biomol. Struct. Dyn. 8*, 491−571.

Hélène, C. (1991) *Anti-Cancer Drug Des. 6*, 569−584.

Ing, N. H., Beekman, J. M., Kessler, D. J., Murphy, M., Jayaraman, K., Zendegui, J. G., Hogan, M. E., O'Malley, B. W., & Tsai, M.-J. (1993) *Nucleic Acids Res. 21*, 2789−2796.

Laughlan, G., Murchie, A. I. H., Norman, D. G., Moore, M. H., Moody, P. C. E., Lilley, D. M. J., & Luisi, B. (1994) *Science 265*, 520−524.

Lu, M., Guo, Q., & Kallenbach, N. R. (1992) *Biochemistry 31*, 2455−2459.

Maher, L. J. (1992) *BioEssays 14*, 807−815.

Maher, L. J., Dervan, P. B., & Wold, B. J. (1990) *Biochemistry 29*, 8820−8826.

Milligan, J. F., Krawczyk, S. H., Wadwani, S., & Matteucci, M. D. (1993) *Nucleic Acids Res. 21*, 327−333.

Moser, H. E., & Dervan, P. B. (1987) *Science 238*, 645−650.

Orson, F. M., Thomas, D. W., McShan, W. M., Kessler, D. J., & Hogan, M. E. (1991) *Nucleic Acids Res. 19*, 3435−3441.

Postel, E. H., Flint, S. J., Kessler, D. J., & Hogan, M. E. (1991) *Proc. Natl. Acad. Sci. U.S.A. 88*, 8227−8231.

Povsic, T. J., & Dervan, P. B. (1989) *J. Am. Chem. Soc. 111*, 3059−3061.

Sen, D., & Gilbert, W. (1990) *Nature 344*, 410−414.

Sen, D., & Gilbert, W. (1992) *Biochemistry 31*, 65−70.

Singleton, S. F., & Dervan, P. B. (1992) *Biochemistry 31*, 10995−11003.

Tabor, C. W., & Tabor, H. (1976) *Annu. Rev. Biochem. 45*, 285−306.

Williamson, J. R., Raghuraman, M. K., & Cech, T. R. (1989) *Cell 59*, 871−880.

BI942043W